

# Original Papers

phys. stat. sol. (a) 66, 45 (1981)

Subject classification: 18.2 and 18.4; 1.1; 22.8

*Institute of Physics, Jagiellonian University, Cracow<sup>1)</sup> (a) and  
Institute of Physics, Technical University of Cracow<sup>2)</sup> (b)*

## Crystal and Magnetic Structure of the $\text{NiMn}_{1-t}\text{Ti}_t\text{Ge}$ System

By

W. BAŻELA (b) and A. SZYTŁA (a)

The magnetic and crystallographic nature of the compounds  $\text{NiMn}_{1-t}\text{Ti}_t\text{Ge}$  ( $0 \leq t \leq 1$ ) are studied by X-ray and neutron diffraction and magnetometric measurements. It is shown that the solid solutions arise for  $0 \leq t \leq 1$ , with the crystal structure of the  $\text{NiTiSi}$  type. A magnetic phase diagram is constructed: for  $0 \leq t \leq 0.1$  helicoidal order exists, for  $0.15 \leq t \leq 0.65$  a non-collinear one.  $\text{NiTiGe}$  is Pauli paramagnetic. The interpretation of the results is performed in terms of a model proposed by Jaccarino and Walker.

Были проведены исследования соединений типа  $\text{NiMn}_{1-t}\text{Ti}_t\text{Ge}$  ( $0 \leq t \leq 1$ ) магнитометрическим методом и методами дифракции нейтронов и рентгеноструктурного анализа. Обнаружено, что существует непрерывный ряд твердых растворов ( $0 \leq t \leq 1$ ) и что все эти соединения обладают кристаллической структурой типа  $\text{NiTiSi}$ . Определена магнитную фазовую диаграмму: соединения с  $0 \leq t \leq 0.1$  имеют геликоидальную магнитную структуру, а соединения с  $0.15 \leq t \leq 0.65$  неколлинеарную структуру. Соединение  $\text{NiTiGe}$  является парамагнетиком Паули. Полученные результаты можно объяснить на основе модели, предложенной Джаккарином и Валькером.

### 1. Introduction

The magnetic properties of the  $\text{MM}'\text{X}$  compounds (with  $\text{M}$ ,  $\text{M}'$  iron group transition elements,  $\text{X}:\text{Si}$ ,  $\text{Ge}$ ) have been investigated for many years [1 to 5]. These compounds have the same orthorhombic  $\text{NiTiSi}$  type structure but they exhibit different magnetic behaviour: 1.  $\text{NiMnGe}$  and  $\text{CoMnSi}$  [1, 2] are antiferromagnetic with helicoidal magnetic structure, 2.  $\text{CoMnGe}$  and  $\text{NiMnSi}$  [3, 4] are collinear ferromagnetics. The difference of the magnetic properties between these compounds seems to be connected with different numbers of the  $(3d + 4s)$  electrons and with interatomic distances. It has stimulated interest in the properties of solid solutions of these compounds.

The present paper describes the results of the magnetic and neutron diffraction investigations of  $\text{NiMn}_{1-t}\text{Ti}_t\text{Ge}$  solid solutions carried out in order to have further understanding of the magnetic properties of these compounds.

### 2. Experimental

#### 2.1 Sample preparation

Stoichiometric amounts of high purity constituent ( $\text{Ni}$ ,  $\text{Mn}$ :  $4N$ ,  $\text{Ti}$ :  $3N$ ,  $\text{Ge}$ :  $5N$ ) were melted together in an argon atmosphere, using an induction furnace. All samples were then annealed in argon filled quartz tubes at 1200 K for 100 h, and cooled to room temperature over a week.

<sup>1)</sup> ul. Reymonta 4, 30-059 Kraków, Poland.

<sup>2)</sup> Podchorążych 1, 30-084 Kraków, Poland.

### 2.2 X-ray studies

X-ray measurements on the powders were carried out using a DRON-1 diffractometer with  $\text{FeK}_\alpha$  radiation. From  $t = 0$  to  $t = 1$  all the lines observed could be indexed in the orthorhombic  $\text{NiTiSi}$ -type structure. A least-squares fit to the observed  $2\theta$  values was used to obtain the lattice parameters. The variations of the lattice parameters with composition are shown in Fig. 1. The  $b$  constants are independent of composition, while the  $a$  and  $c$  constants exhibit a jump in the region  $0.4 \leq t \leq 0.5$ .

### 2.3 Magnetic macroscopic measurements

Low field magnetometric measurements (up to 1.0 T) were carried out in temperatures ranging from 100 to 600 K, using an electronic balance.

The measurements in strong magnetic fields (up to 15 T) for the samples with  $t = 0, 0.05, 0.1, 0.25$  were performed with a pulse magnetometer of conventional design [6] at temperature of 80 K.

The magnetization and reciprocal magnetic susceptibility versus temperature curves are shown in Fig. 2.

For the samples with  $t = 0.05$  and  $0.1$  the temperature dependences of magnetic susceptibility have apparent maxima at the Néel temperature. The jump of the temperature dependence of susceptibility for the sample with  $t = 0.05$  at  $T_{\text{tm}} = 200$  K (similar as  $\text{NiMnGe}$ ) on heating proves the existence of an additional phase transition.

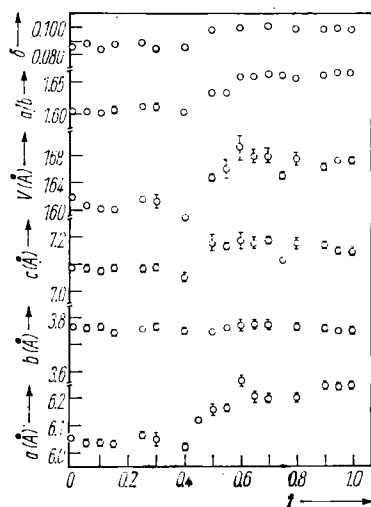


Fig. 1

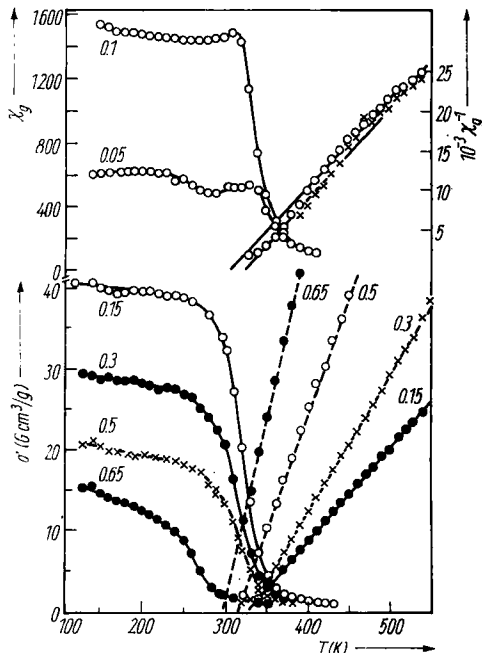


Fig. 2

Fig. 1. The variation of the lattice parameters, the unit cell volume, the  $a/b$  ratio, and deformation parameter  $\delta = (c/\sqrt{3}b) - 1$ , as functions of composition for the  $\text{NiMn}_{1-t}\text{Ti}_t\text{Ge}$  system

Fig. 2. Results of magnetic measurements for the  $\text{NiMn}_{1-t}\text{Ti}_t\text{Ge}$  system

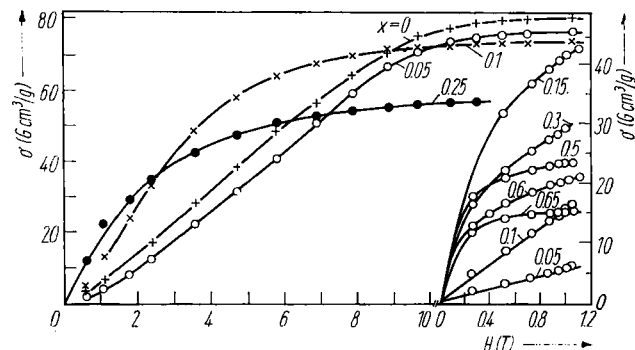


Fig. 3. High field magnetization curves of  $\text{NiMn}_{1-t}\text{Ti}_t\text{Ge}$  ( $t = 0, 0.05, 0.1, 0.25$ ) at 80 K. The same dependence in a weak magnetic field is also shown

For the samples with  $0.15 \leq t \leq 0.65$  a spontaneous magnetization is observed at low temperatures (see Fig. 2). The values of magnetization decrease with increasing  $t$ .

For the samples with  $0.7 \leq t \leq 0.95$  the reciprocal susceptibility obeys the Curie-Weiss law at high temperatures. The deviation from Curie-Weiss law observed at low temperatures is connected with some ferromagnetic impurity.

The magnetization curves up to 15 T obtained at 80 K are shown in Fig. 3. As it is seen from the figure, the magnetization curves for samples with  $t = 0, 0.05$ , and  $0.1$  indicate their metamagnetic nature. The same dependences in weak magnetic fields for the samples with concentrations  $0.15 \leq t \leq 0.65$  are also shown. For the samples with  $t = 0.05$  and  $0.1$  the magnetization is linear, while for the compounds with  $0.15 \leq t \leq 0.65$  the magnetization curves have ferromagnetic character but do not attain saturation in the magnetic field of  $H = 1$  T.

Table 1  
The results of magnetometric measurements for the  $\text{NiMn}_{1-t}\text{Ti}_t$  system

$t$	$T_N, T_C$ (K)	$\theta_p$ (K)	$\mu_{\text{eff}} (\mu_B)$ per formula unit
0	346	277	4.3
0.05	333	308	3.85
0.10	318	332	3.55
0.15	335	340	3.35
0.20	330	332	3.00
0.25	331	327	3.06
0.30	331	331	3.00
0.40	320	319	2.60
0.50	328	325	2.30
0.55	322	330	2.15
0.60	331	331	2.00
0.65	282	300	1.80
0.70		252	2.00
0.75		278	2.00
0.80		75	1.90
0.90		194	1.30
0.95		208	1.00

For NiTiGe the magnetometric measurements were performed from 4.2 K to room temperature. The susceptibility does not reveal any temperature dependence. The  $\chi(T)$  diagrams are typical for Pauli paramagnetics.

The Néel or Curie temperatures, the asymptotic Curie-Weiss temperatures  $\theta_p$ , as well as the magnetic moment values in paramagnetic state were established from these measurements. The results are given in Table 1. The values of the Néel temperatures decrease with increasing  $t$ . The Curie temperatures are constant. The positive values of  $\theta_p$  suggest that a ferromagnetic interaction becomes dominant. The magnetic moment per formula unit in the paramagnetic state decreases with increase in  $t$ .

In order to estimate the magnetic structures of these compounds neutron diffraction experiments were performed.

#### 2.4 Neutron diffraction experiment

Neutron diffraction measurements were made on powder samples (for  $t = 0.05, 0.1, 0.15, 0.25$ , and  $1.0$ ) at the reactor in the Boris Kidrič Institute in Vinča. The diffraction patterns for the sample  $t = 0.05$ , are shown in Fig. 4.

##### 2.4.1 Determination of crystal structure using neutron diffraction

The analysis of the nuclear diffraction intensities confirm that the compounds are isostructural with NiTiSi type structure. In this structure the atoms of each kind occupy their own position 4 (c) in the space group Pnma,

$$x, \frac{1}{4}, z, \bar{x}, \frac{3}{4}, \bar{z}, \frac{1}{2} - x, \frac{3}{4}, \frac{1}{2} + z, \frac{1}{2} + x, \frac{1}{4}, \frac{1}{2} - z.$$

The positional parameters  $x$  and  $z$  determined from nuclear reflections by the profile refinement method [7] are given in Table 2. The nuclear scattering lengths were taken from the table published in [8].

##### 2.4.2 The magnetic structure determined by neutron diffraction measurements

In the diagrams for samples with  $t = 0.05, 0.1$  at 80 and 295 K extra peaks of magnetic origin were visible. All peaks were indexed by assuming the propagation vector  $\mathbf{k} = (\tau, 0, 0)$ . The values of  $\tau$  decrease with increase in  $t$ . From the analysis of magnetic peak intensities, the following models of helicoidal magnetic structure were suggested:

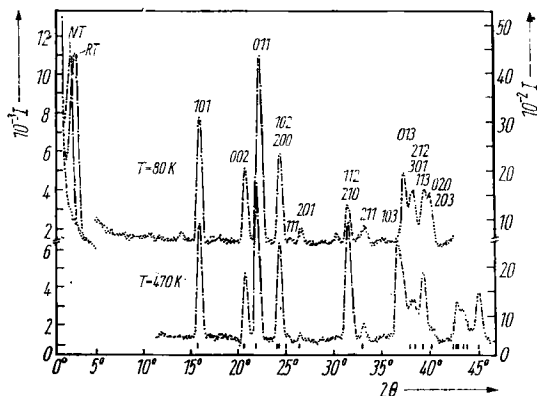


Fig. 4. Neutron diffraction patterns of  $\text{NiMn}_{0.95}\text{Ti}_{0.05}\text{Ge}$  at 80 and 470 K ( $\lambda = 1.284 \text{ \AA}$ )

Table 2  
Unit cell dimensions and position parameters for the  $\text{NiMn}_{1-t}\text{Ti}_t\text{Ge}$  system corresponding to the space group Pnma\*)

<i>t</i>	0.05		0.1		0.15		0.25		1.0	
	<i>T</i>	80 K	470 K	80 K	110 K	373 K	100 K	293 K	100 K	293 K
<i>a</i> (Å)	6.038(3)	6.042(2)	6.045(2)	6.061(5)	6.077(3)	6.087(8)	6.244(2)	6.244(2)	6.244(2)	6.244(2)
<i>b</i> (Å)	3.736(1)	3.794(1)	3.733(1)	3.750(2)	3.807(2)	3.747(4)	3.747(1)	3.747(1)	3.747(1)	3.747(1)
<i>c</i> (Å)	7.032(3)	7.063(3)	7.069(3)	7.077(7)	7.079(6)	7.079(6)	7.112(9)	7.147(2)	7.147(2)	7.147(2)
<i>V</i> (Å <sup>3</sup> )	159.771(8)	161.891(4)	159.52(12)	160.87(35)	163.77(22)	163.77(22)	162.24(55)	167.20(10)	167.20(10)	167.20(10)
Ni <i>x</i>	0.142(1)	0.153(1)	0.147(1)	0.137(2)	0.148(1)	0.148(1)	0.134(2)	0.141(1)	0.141(1)	0.141(1)
Ni <i>z</i>	0.569(1)	0.553(1)	0.560(1)	0.556(2)	0.558(1)	0.558(1)	0.552(2)	0.560(1)	0.560(1)	0.560(1)
Mn } <i>x</i>	0.038(3)	0.029(4)	0.031(2)	0.040(5)	0.031(4)	0.031(4)	0.032(3)	0.032(3)	0.032(3)	0.032(3)
Ti } <i>z</i>	0.290(3)	0.180(4)	0.176(2)	0.209(6)	0.209(4)	0.209(4)	0.202(6)	0.187(3)	0.187(3)	0.187(3)
Ge <i>x</i>	0.762(1)	0.768(2)	0.758(1)	0.760(3)	0.763(2)	0.763(2)	0.746(4)	0.758(2)	0.758(2)	0.758(2)
Ge <i>z</i>	0.624(1)	0.624(1)	0.626(1)	0.634(2)	0.634(1)	0.634(1)	0.621(3)	0.623(1)	0.623(1)	0.623(1)
<i>R</i> (%)	3.8	4.9	5.5	7.6	6.1	4.5	11.8	4.5	4.5	4.5

\*) Standard deviations based on statistics only are given in parentheses.

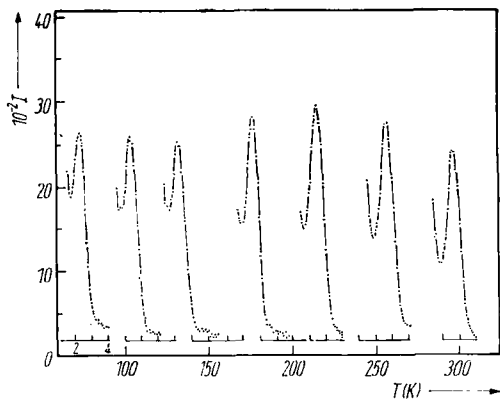


Fig. 5. Temperature dependence of the intensities  $I$  of the  $(000)^\pm$  reflection for  $\text{NiMn}_{0.95}\text{Ti}_{0.05}\text{Ge}$

for sample  $t = 0.05$ , at  $T < T_{\text{tm}}$  the spiral axis is parallel to the  $c$ -axis (cycloidal spiral),  $\tau = 0.187$ ,  $\mu_{\text{Mn}} = (2.59 \pm 0.05) \mu_{\text{B}}$ , at  $T_{\text{tm}} < T < T_{\text{N}}$  the spiral axis lies along the  $a$ -axis (simple spiral),  $\tau = 0.22$ ,  $\mu_{\text{Mn}} = (2.0 \pm 0.1) \mu_{\text{B}}$ ;

for  $t = 0.1$  at all temperatures the simple spiral is observed,  $\tau = 0.145$ ,  $\mu_{\text{Mn}} = (2.4 \pm 0.2) \mu_{\text{B}}$  at  $T = 80$  K.

For the sample with  $t = 0.05$  additional measurements were made in the temperature range 80 to 293 K in order to see the influence of temperature on the spiral structure. The temperature dependence of the intensity for the  $(000)^\pm$  reflection has been measured (see Fig. 5). A strong increase in the reflection intensity, connected with the reorientation of the spiral axis, is observed at 200 K.

In the case of the samples with  $t = 0.15$  and 0.25 no extra reflections appear. Only an increase in the intensities of the fundamental reflections is observed indicating that the unit cell has not changed. The analysis using the space group representations method [9] gives eight possible magnetic structures:  $\text{F}_z\text{C}_x$ ,  $\text{F}_x\text{C}_z$ ,  $\text{F}_y$ ,  $\text{C}_y$ ,  $\text{A}_z\text{G}_z$ ,  $\text{A}_z\text{G}_x$ ,  $\text{A}_y$ ,  $\text{G}_y$ , where

$$\text{F} = \text{S}_1 + \text{S}_2 + \text{S}_3 + \text{S}_4, \quad \text{G} = \text{S}_1 - \text{S}_2 + \text{S}_3 + \text{S}_4,$$

$$\text{C} = \text{S}_1 + \text{S}_2 - \text{S}_3 - \text{S}_4, \quad \text{A} = \text{S}_1 - \text{S}_2 - \text{S}_3 + \text{S}_4.$$

The numbers of atoms are given in Section 2.4.1.

The calculation based on the profile refinement method [7] gives results consistent only with the  $\text{F}_z\text{C}_x$  model. The obtained magnetic moment components of Mn atoms are as follows:

$$\mu_x = (1.8 \pm 0.3) \mu_{\text{B}}, \quad \mu_z = (2.5 \pm 0.6) \mu_{\text{B}}, \quad \mu_{\text{tot}} = (3.1 \pm 0.5) \mu_{\text{B}} \quad \text{for } t = 0.15,$$

$$\mu_x = (1.0 \pm 0.5) \mu_{\text{B}}, \quad \mu_z = (2.5 \pm 0.7) \mu_{\text{B}}, \quad \mu_{\text{tot}} = (2.7 \pm 0.7) \mu_{\text{B}} \quad \text{for } t = 0.25.$$

### 3. Discussion

The magnetic phase diagram of the system  $\text{NiMn}_{1-t}\text{Ti}_t\text{Ge}$  derived on the basis of magnetometric and neutron diffraction measurements is shown in Fig. 6.

In the system  $\text{NiMn}_{1-t}\text{Ti}_t\text{Ge}$  the magnetic moments are localized only on Mn atoms. The magnetic interactions between neighbouring Mn atoms are presented in Fig. 7.

Taking into account the Mn atom distribution in the unit cell and the Goodenough-Kanamori rules [10, 11], the following exchange integrals were obtained for  $\text{NiMnGe}$ :  $J_{11} \leqq 0$ ,  $J_{12} \geqq 0$ ,  $J_{12} \approx 0$ ,  $J_{13} < 0$ ,  $J_{14} \leqq 0$ . These exchange integrals are in agreement

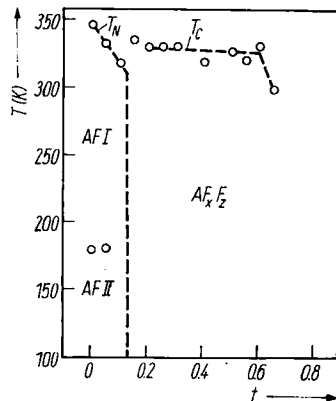


Fig. 6

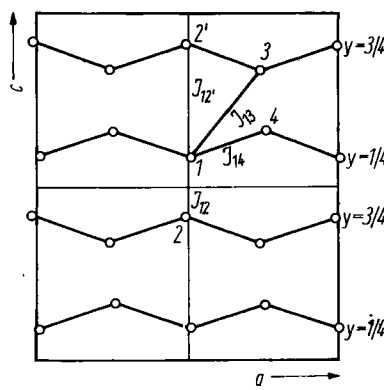


Fig. 7

Fig. 6. Magnetic phase diagram of the  $\text{NiMn}_{1-t}\text{Ti}_t\text{Ge}$  system. (AFI simple spiral, AFII cycloidal spiral,  $\text{AF}_x\text{F}_z$  noncolinear structure)

Fig. 7. Magnetic interactions between neighbouring Mn atoms in the  $\text{NiMnGe}$  structure

with the determined magnetic structure, which consists of ferromagnetic planes perpendicular to the  $a$ -axis (for the temperatures  $T_{\text{tm}} < T < T_{\text{N}}$ ).

The dilution of the Mn sublattice by Ti atoms in the  $\text{NiMn}_{1-t}\text{Ti}_t\text{Ge}$  compounds leads to a diminution of magnetic interactions.

In terms of a model proposed by Jaccarino and Walker [12] the decrease in moment with decreasing  $y$  ( $y = 1 - t$ ) can be ascribed to a loss of moment in those Mn atoms which have an insufficient number of Mn atoms as nearest neighbours. For each concentration  $y$  the probability of Mn atoms having  $n$  Mn atoms as nearest neighbours, out of a maximum number of  $N$  is given by

$$P(y, n, N) = \frac{N!}{n!(N-n)!} y^n (1-y)^{N-n}.$$

The number  $N$  is determined by the crystal structure.  $N = 6$  was assumed taking into account all neighbours at a distance less than 4 Å. The function  $P(y, n, N)$  is drawn in Fig. 8 for different  $y$ . The maximum in  $P(y, n, 6)$  for  $y = 0.95$  and  $y = 0.9$  appears at  $n = 6$ , and for  $y = 0.85$  at  $n = 5$ . It was stated that the magnetic structure changes at  $y = 0.85$  ( $t = 0.15$ ). This fact leads to the conclusion that the lack of one interaction is responsible for the change of structure.

A Mn atom takes part in the magnetic interactions if it is surrounded by at least  $j$  Mn neighbours. If so, the value of the average moment can be approximated by the following formula:  $\mu(y) = y P_j(y) \mu(y=1)$ , where  $P_j(y) = \sum_{n=j}^N P(y, n, N)$ .

Results of the calculations performed on the assumption that there are at least 2, 3, and 4 Mn neighbours are shown in Fig. 9 (curves 1, 2, 3, respectively). The values of the magnetic moment, as yielded by magnetometric and neutron diffraction methods, are also displayed on Fig. 9. The curve 2 provides the best fit to the experimental data. This means that at least three other Mn atoms are needed in the nearest neighbourhood in order to allow an Mn atom to share magnetic ordering.

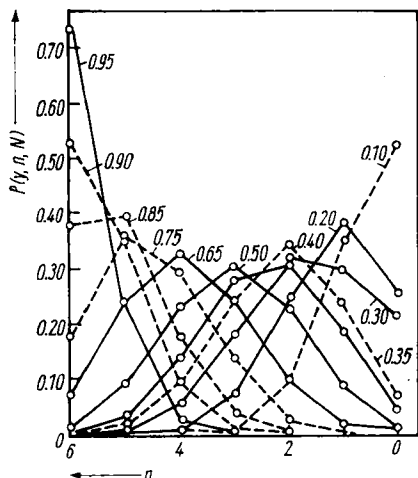


Fig. 8

Fig. 8. The function  $P(y, n, N)$  calculated for different  $y$  for the  $\text{NiMn}_y\text{Ti}_{1-y}\text{Ge}$  system

Fig. 9. Concentration dependence of the saturation moment in the  $\text{NiMn}_y\text{Ti}_{1-y}\text{Ge}$  system. The full lines represents the calculated values (see text);  $\circ$  magnetometric and  $\Delta$  neutron diffraction measurements

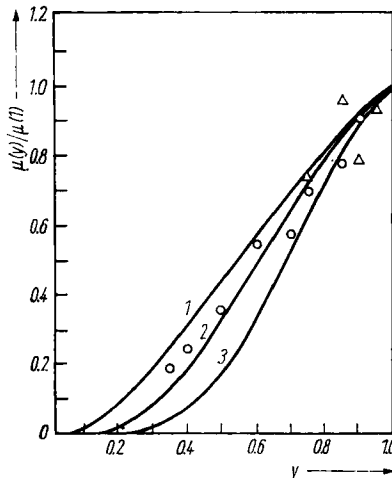


Fig. 9

#### Acknowledgements

The authors are grateful to the Polish Academy of Sciences for financial support and Dr. A. Zięba for magnetization measurements in strong magnetic fields. The authors would like to express their gratitude to the staff of the Laboratory of Solid State Physics, Boris Kidrič Institute at Vinča.

#### References

- [1] W. BAŻELA, A. SZYTUŁA, J. TODOROVIĆ, Z. TOMKOWICZ, and A. ZIĘBA, phys. stat. sol. (a) **38**, 721 (1976).
- [2] S. NIZIOL, H. BIŃCZYCKA, A. SZYTUŁA, J. TODOROVIĆ, R. FRUCHART, J. P. SENATEUR, and D. FRUCHART, phys. stat. sol. (a) **45**, 591 (1978).
- [3] V. JOHNSON and C. G. FREDERICK, phys. stat. sol. (a) **20**, 331 (1973).
- [4] V. JOHNSON, Inorg. Chem. **14**, 1117 (1975).
- [5] S. ANZAI and K. OZAWA, Phys. Rev. B **18**, 2173 (1978).
- [6] S. NIZIOL, A. ZIĘBA, and J. KULKA, Sci. Bull. Acad. Mining and Metallurgy, No. 483, Cracow 1975.
- [7] H. M. RIETVELD, J. appl. Cryst. **2**, 65 (1969).
- [8] G. E. BACON, Acta cryst. **A28**, 357 (1972).
- [9] E. F. BERTAUT, Acta cryst. **A24**, 217 (1968).
- [10] J. B. GOODENOUGH, Magnetism and the Chemical Bond, Interscience Publishers, New York 1966.
- [11] J. KANAMORI, J. Phys. Chem. Solids **10**, 87 (1959).
- [12] V. JACCARINO and L. R. WALKER, Phys. Rev. Letters **15**, 259 (1965).

(Received December 8, 1980)